Received: 12 March 2022 | Revised: 2 October 2022 | Accepted: 8 November 2022

DOI: 10.1111/wrr.13059

ORIGINAL ARTICLE - BASIC SCIENCE

Wound Repair and Regeneration — WILEY

Comparison of biopolymer scaffolds for the fabrication of skin substitutes in a porcine wound model

Bronwyn L. Dearman BSc(Hons), PhD[1,2,3] | **Steven T. Boyce PhD**[4] | **John E. Greenwood BSc(Hons), MBChB, MD, DHlthSc, FRCS(Eng), FRCS(Plast), FRACS**[2]

[1]Skin Engineering Laboratory, Adult Burns Centre, Royal Adelaide Hospital, Adelaide, South Australia, Australia

[2]Adult Burns Centre, Royal Adelaide Hospital, Adelaide, South Australia, Australia

[3]Faculty of Health and Medical Science, The University of Adelaide, Adelaide, South Australia, Australia

[4]Department of Surgery, University of Cincinnati, Cincinnati, Ohio, USA

Correspondence
Bronwyn L. Dearman, Royal Adelaide Hospital, 1 Port Road, Adelaide, SA 5000, Australia.
Email: bronwyn.dearman@sa.gov.au

Funding information
Lifetime Support Authority, Grant/Award Number: GA00061

Abstract

This study compared three acellular scaffolds as templates for the fabrication of skin substitutes. A collagen-glycosaminoglycan (C-GAG), a biodegradable polyurethane foam (PUR) and a hybrid combination (PUR/C-GAG) were investigated. Scaffolds were prepared for cell inoculation. Fibroblasts and keratinocytes were serially inoculated onto the scaffolds and co-cultured for 14 days before transplantation. Three pigs each received four full-thickness 8 cm × 8 cm surgical wounds, into which a biodegradable temporising matrix (BTM) was implanted. Surface seals were removed after integration (28 days), and three laboratory-generated skin analogues and a control split-thickness skin graft (STSG) were applied for 16 weeks. Punch biopsies confirmed engraftment and re-epithelialisation. Biophysical wound parameters were also measured and analysed. All wounds showed greater than 80% epithelialisation by day 14 post-transplantation. The control STSG displayed 44% contraction over the 16 weeks, and the test scaffolds, C-GAG 64%, Hybrid 66.7% and PUR 67.8%. Immunohistochemistry confirmed positive epidermal keratins and basement membrane components (Integrin alpha-6, collagens IV and VII). Collagen deposition and fibre organisation indicated the degree of fibrosis and scar produced for each graft. All scaffold substitutes re-epithelialised by 4 weeks. The percentage of original wound area for the Hybrid and PUR was significantly different than the STSG and C-GAG, indicating the importance of scaffold retainment within the first 3 months post-transplant. The PUR/C-GAG scaffolds reduced the polymer pore size, assisting cell

Abbreviations: BM, basement membrane; BTM, biodegradable temporising matrix; CCS, composite cultured skin; C-GAG, collagen-glycosaminoglycan scaffolds; DAB, 3,3′-diaminobenzidine; DAWE, Australian Government Department of Agriculture, Water and the Environment; EI, erythema index; H&E, haematoxylin and eosin; HRP, horseradish peroxidase; IHC, immunohistochemistry; LBL, layer by layer; MI, melanin index; MVD, microvessel density; OCT, optimal cutting temperature embedding medium; PCL, polycaprolactone; pFbs, porcine fibroblasts; pFFP, porcine fresh frozen plasma; pKs, porcine keratinocytes; PLA, polylactic acid; PLGA, poly(lactide-co-glycolide); PSR, picrosirius red stain; PUR, polyurethane; PVA, polyvinyl alcohol; PVP, polyvinylpyrrolidone; SAHMRI, South Australian Health and Medical Research Institute; STSG, split-thickness skin graft; TEWL, transepidermal water loss; VE, viscoelasticity.

retention and reducing the contraction of in vitro collagen. Further investigation is required to ensure reproducibility and scale-up feasibility.

KEYWORDS
biopolymers, burns, porcine wound model, scaffolds, skin substitutes

1 | INTRODUCTION

In the last decade, transformative technologies have emerged and expanded the interest in tissue engineered skin substitutes. However, a cost-effective, clinically available, dermal-epidermal tissue-engineered skin substitute still remains elusive due to the complexity, high cost and time-consuming nature of production.[1] Several limitations exist with the current dermal scaffold models used to generate engineered skin substitutes. Most experience since 1975 has been with utilising animal-derived collagens and combinations such as collagen/glycosaminoglycan (C-GAG).[2–4] Since the dermis lost to burn injury is composed of these biopolymers, replacement with like as a scaffold for autologous cellular delivery seems intuitive, although xenogeneic collagens are costly and have potential immunogenicity and concerns of disease transmission. Despite clinical success,[5] these scaffolds and subsequent grafts have been shown to contract to 50% of their original area in vitro, and have the potential to alter mechanical properties.[6] Recently, experience with synthetic polymers as scaffolds has been published, demonstrating successful incorporation into a skin substitute model,[7] even indicating apparent advantages over collagen-based scaffolds,[8] albeit with limitations. There are few substitutes that constitute only a scaffold without additional materials. Some synthetic polymers' degradation products and residual additives are cytotoxic or fail to degrade completely.[9] Polyethylene glycol, polyurethanes (PUR), polyvinyl alcohol (PVA), polylactic acid (PLA), polycaprolactone (PCL),[10,11] polyvinylpyrrolidone (PVP),[12] poly(lactide-co-glycolide) (PLGA)[13] and polystyrene[14] have all received attention. Whether consisting of electrospun or woven fibres or having a foam structure, the pores are not uniform and have a broad range of sizes and an unpredictable proportion of open or closed cells. Pore size variability, mainly if they are large, decreases the mechanical stability of the overall structure and cell retention,[15] although diameters of greater than 500 μm might aid rapid vascularisation.[16] If the pores are too small, they inhibit cellular ingrowth and collagen deposition. Some iterations of tissue scaffolds use a combination of biological and synthetic polymers to generate an extracellular matrix that mimics the dermal fibrous structure by increasing cellular recognition and tissue compatibility. These have included fibrin hydrogels, gelatin, sodium alginate, hyaluronic acid (HA), amniotic membrane and silk.[8,17–24] These can assist with porosity whilst providing a microenvironment that supports epidermal integrity.

The potential of a PUR generated composite cultured skin (CCS) in a porcine wound model in small and large wounds has been demonstrated.[7,25,26] However, PUR batch consistency has plagued production with an unacceptable proportion of pores exceeding 1 mm diameter. The CCS consists of a PUR foam scaffold soaked in fresh frozen plasma and human thrombin to produce a fibrin network, reducing the polymer pore sizes. This gelation reduces fibroblast loss and increases keratinocyte retention on an external surface during and after inoculation. Although this method has shown clinical success with previous PUR foam iterations, the additives inherently introduce variability and batch to batch inconsistency. A ready-to-use, off-the-shelf product is desirable. Since collagen-GAG has an experimental and clinical history, it was postulated that a PUR/C-GAG hybrid might provide advantages from both materials—simultaneously filling the oversized pores of the PUR foam with C-GAG to afford greater cellular retention post-inoculation and promotion of epidermal morphogenesis. The PUR scaffold provides additional structural support to reduce C-GAG contraction. This report describes a comparison among these three scaffolds against each other and a skin-graft control to generate a bi-layered skin substitute for extensive full-thickness burns. The investigators believe this is the first hybrid scaffold composed of PUR foam and collagen-GAG scaffold that has been evaluated in a large animal model.

2 | MATERIALS AND METHODS

2.1 | Scaffolds

The biodegradable polyurethane (PUR) NovoSorb® foam is 1 mm thick for CCS production. PUR scaffolds for both in vitro and in vivo experiments were cut to size from sterile 24.5 cm × 24.5 cm ± 0.3 cm sheets. The collagen-glycosaminoglycan (C-GAG) scaffolds were bovine dermal collagen and chondroitin-6-sulphate from shark cartilage and fabricated as per Boyce et al. 1988 (kindly provided from the Boyce Lab, Cincinnati). These were dry-packed, sterile ~8 cm × 8 cm pieces. The hybrid (PUR/C-GAG) was formulated using 1 mm PUR sheets and liquid C-GAG. The C-GAG permeated the PUR overnight and was then processed as per Boyce et al. 1988.[3] The cross-linking step of thermal hydration was replaced by direct chemical cross-linking in 30 mM 1-Ethyl-3-(3-dimethylaminopropyl) carbodiimide hydrochloride (EDC) as per Powell and Boyce.[27] All scaffolds were sterilised by gamma-irradiation.

2.2 | Animal model

Three large white × Landrace pigs were used, average weight 27 kg upon BTM implantation. Approval was granted by the South

Australian Health and Medical Research Institute (SAHMRI) Animal Ethics Committee (Approval number SAM282v4). Due to the use of bovine collagen from the USA, additional approval from the Australian Government Department of Agriculture, Water and the Environment (DAWE) was necessary for the in vivo use of a restricted imported biological material (Approval #2019/081). All animals were humanely treated and were acclimatised for 11 days. Four days prior to surgery, one unit of blood (~400 ml) was collected from each pig by jugular venipuncture to isolate autologous porcine fresh frozen plasma (pFFP) for PUR substitute fabrication. On the day of surgery, general anaesthesia was induced with intramuscular Ketamine-Xylazine (Ketamine 10 mg/kg, Xylazine 2 mg/kg) 30 min before intubation with IM Noroclav (amoxicillin/clavulanic acid—1 ml/20 kg) administered once anaesthetised. Post-operative pain was managed with 1 ml of Buprenorphine Hydrochloride (324 μg) administered subcutaneously on anaesthetic recovery and for the next 3 days with a single 2 μg/kg/h Fentanyl patch.

2.3 | Wound administration (BTM implantation)

The wounds were generated, prepared and dressed according to our previous studies.[7,25,26] In brief, four full-thickness 8 cm × 8 cm surgical wounds were created to the level of the panniculus adiposus. The excised skin provided the source of autologous cells for individual substitute fabrication. NovoSorb™ Biodegradable Temporising Matrix (BTM) was cut to size and implanted, affixed with staples and allowed to integrate for 28 days. The wounds were monitored, measured, photographed and re-dressed twice weekly.

2.4 | Fabrication of skin substitutes

On the day of BTM implantation, the four pieces of excised skin per pig were processed for autologous cell isolation. On average, this totalled 195cm^2 per pig. Porcine fibroblasts (pFbs) and porcine keratinocytes (pKs) were cultured as per Dearman et al. 2013, 2014, 2021.[7,25,26] Cells were expanded and then cryopreserved (Coolcell, Corning, Australia) until required for pending skin substitute setup. Duplicate substitutes were established for each pig, except C-GAG (where triplicates were required). Three days prior to pFbs inoculation, PUR foams were soaked in autologous pFFP. One day prior, the C-GAGs underwent pre-washing along with hybrid cross-linking. A double-layering method (LBL) of plasma/thrombin was used for the PUR. pFbs were inoculated on day 0 at 7.5 × 10^5/cm^2 and pKs 3 days later at 1 × 10^6/cm^2. All substitutes were cultured at an air-liquid interface, and media were exchanged daily as previously described.[28] The skin substitutes were incubated at 37°C, 5% CO_2, saturated humidity for 14 days until their application 28 days after the implanted BTMs. To prepare the sites for graft transplantation, BTM seals were delaminated and lightly dermabraded to generate punctate bleeding. The skin substitutes were then cut to size and applied with a piece of Mepitelone cut 1 cm larger than the graft to aid transfer to the wound site.

Split-thickness skin graft (STSG), meshed 1:3, were used as controls to replicate a typical mesh size employed for extensive burns. A Zimmer® Electric Dermatome (kindly loaned by Zimmer Pty Ltd), set at 0.012 inches, enabled a clean ~5 cm × 9 cm graft from the top right shoulder area. This graft was meshed, applied to wounds and secured with staples.

2.5 | Qualitative wound analysis

Wounds were maintained and dressed as previously described.[7] The DermaLab Combo (Cortex, Hadsund, Denmark) readings were performed at weeks 2, 4, 8, 12 and 16. Three-mm punch biopsies were collected and fixed in 10% neutral buffered formalin for paraffin embedding. Fresh frozen samples were placed in cryoprotectant OCT™ embedding medium (ProSciTech, QLD, Australia) in plastic moulds, frozen in isopentane cooled to freezing point, and stored at −80°C. The wound area and biopsy locations was traced onto sterile acetate sheets for map tracing. ImageJ analysis of wound area was performed by taking two ruler measurements top and bottom of the wound, averaging them, scale set and area determined. Epithelialisation and engraftment were defined by a visible epidermal matte layer on the wound surface. The percentage of re-epithelialisation and original wound area were determined over time.

2.5.1 | Histological evaluations

Post fixation, paraffin-embedded biopsies were processed for routine histology, cut at 5–7 μm, and stained with haematoxylin and eosin (H&E). Three biopsies were taken for each condition at each timepoint for histological analysis. Immunohistochemical (IHC) staining on paraffin and frozen sections confirmed the epidermal and dermal anatomy. Frozen sections were air-dried at room temperature for 1 h before a 10-min acetone fixation step followed by standard immunofluorescence. Paraffin sections were processed using a Mouse and Rabbit specific HRP/DAB IHC micro polymer detection kit (ab236466, Abcam) or a streptavidin-biotinylated immunoperoxidase technique.[29] For immunofluorescence, primary and secondary antibodies are detailed in Supporting Information tables. Images were captured with an Olympus FV3000 confocal microscope and scanned with a Zeiss Axio Scan.Z1 slide scanner (Carl Zeiss, Germany). Control tissues were normal human skin from donors undergoing elective surgery procedures, or normal porcine skin from healthy, species matched pigs. Picrosirius red (PSR) stain (ab150681, Abcam) was used to determine and visualise collagen deposition, fibre orientation and organisation. Samples were taken on days 10, 21, 56 and 112 for each condition. Representative slides were imaged using polarising light microscopy (Zeiss, Axio Scan.Z1 slide scanner, Germany) to detect birefringence. Collagen type 1 (thick fibres) stains yellow/orange birefringence, and collagen III (thin fibres) stain green birefringence. Microvascular density (MVD) was assessed for endothelial cell marker CD31, positive

neovessels were stained with 3,3′-diaminobenzidine (DAB), and Ki67 was used as a cellular marker to assess Ki67+ expression and proliferation.

2.6 | Ordinal and quantitative wound assessment

2.6.1 | Observer Scar Assessment Scale (OSAS)

The POSAS[30] observer scale was modified as a scar assessment tool for the final study time point. This scale measures the overall vascularity, pigmentation, thickness, relief, pliability, and site surface area. These were scored on a scale ranging from 1 ('like normal skin') to 10 ('very different from normal skin'), with an overall observer opinion. The total score was calculated for each condition. Ratings from animal subjects could not be recorded.

2.6.2 | DermaLab

The Transepidermal Water Loss (TEWL) probe is an open chamber method based on Nilsson's Vapor Pressure gradient (Cortex, DermaLab). Light to moderate pressure was applied against the skin. In addition to measuring TEWL, the other DermaLab probes evaluated skin elasticity, skin colour and skin thickness. Measurements were performed in triplicate, except for the skin elasticity probe (single sample), as this requires a 45-minute rest period between each measurement cycle. Environmental temperature and humidity were recorded for all measurements. Viscoelasticity (VE—MPa), Melanin Index (MI) and Erythema Index (EI) were parameters chosen for evaluation. The DermaLab calculates the VE by combining the elasticity modulus and the retraction phase. The same investigator performed all the measurements at all timepoints

2.7 | Statistical analyses

Wound area percentage over time was assessed using linear mixed-effects modelling, with fixed effects for test conditions (STSG, C-GAG, PUR, PUR/C-GAG), time in days and the reciprocal of time in days. Two-way interactions between condition and time and the reciprocal of time were included to enable the effect of time on wound area to vary according to condition. A random effect for each animal was specified to account for repeated measurements made on the same pigs. Mean wound percentage for each condition at selected time points were estimated post-hoc, and pairwise comparisons of wound area percentage between and among conditions were conducted at 14, 28 and 112 days. The Bonferroni adjustment for multiple comparisons was applied, a p-value of <0.05 was considered statistically significant. The charts displayed show the observed values with mean and standard deviation for each outcome. In addition, a Friedman test was conducted on three pigs to examine the effect of condition on OSAS score. Each pig was subjected to each of five conditions. Pairwise comparisons of interest were assessed using Wilcoxon matched-pairs signed-rank tests, adjusted for multiple comparisons using the Bonferroni correction. All analyses were performed using Stata v15 (College Station, TX, USA).

3 | RESULTS

3.1 | In vitro observations of skin substitutes

Prior to the commencement of the in vivo study, PUR, C-GAG and hybrid models showed histological evidence of an organised epidermal-dermal composite suitable for transplant (Figure S1). In vitro contraction of C-GAG scaffolds showed a mean percentage decrease of 55% from dry state to cellular inoculation ($n = 9$). The hybrid (PUR/C-GAG) and PUR scaffold resulted in no contraction. A decrease of cross-linked C-GAG in hybrid scaffolds was observed in histological sections, causing non-homogenous epidermal integrity.

3.2 | Macroscopic observations

The BTM integrated into wounds with minimal delamination of the surface seals and only contracted 3.6% of the original wound area until transplantation. Biopsies post-delamination and pre-dermabrasion showed well-integrated polymer adjacent to the subcutaneous fat with a small granulation layer supra.

The C-GAG grafts were fragile and thin to manipulate, requiring multiple staples to piece together and achieve wound area coverage. The hybrid graft was the easiest to cut, handle and apply, followed closely by the PUR scaffold graft. There was no evidence of gross infection in any conditions with minimal scratching observed; all pigs were healthy for the entirety of the study, and upon complete healing, all wounds remained closed for the observation period. Representative images of wounds and conditions from selected time points post-transplantation at days 0, 14, 28, 56 and 112 (2, 4, 8, 16 weeks) are shown in Figure 1A–D. The final percentage of wound contraction from original is tabled in Figure 1E for each condition.

The 1:3 meshed STSG engrafted by day 14 with 100% wound re-epithelialisation. The PUR substitute displayed a dry superficial crust-like appearance over a large percentage of the wound, and with gentle removal, the wound was fully re-epithelialised below with a developed epidermal barrier. Hybrid grafts showed initial engraftment with small areas of PUR scaffold extrusion 2 weeks post-transplant with secondary re-epithelialisation assisting complete closure. The C-GAG substitutes displayed interstitial healing. A small area of graft detachment and loss was observed, and a serous collection was extracted to enable reattachment.

The percentage of wound area from the original showed significant differences ($p < 0.05$) for all skin substitute conditions compared with the STSG for all time points measured. No differences ($p > 0.05$) were observed among the three test conditions by study end (Figure 2A). On day 28 post-transplant, the percentage of original

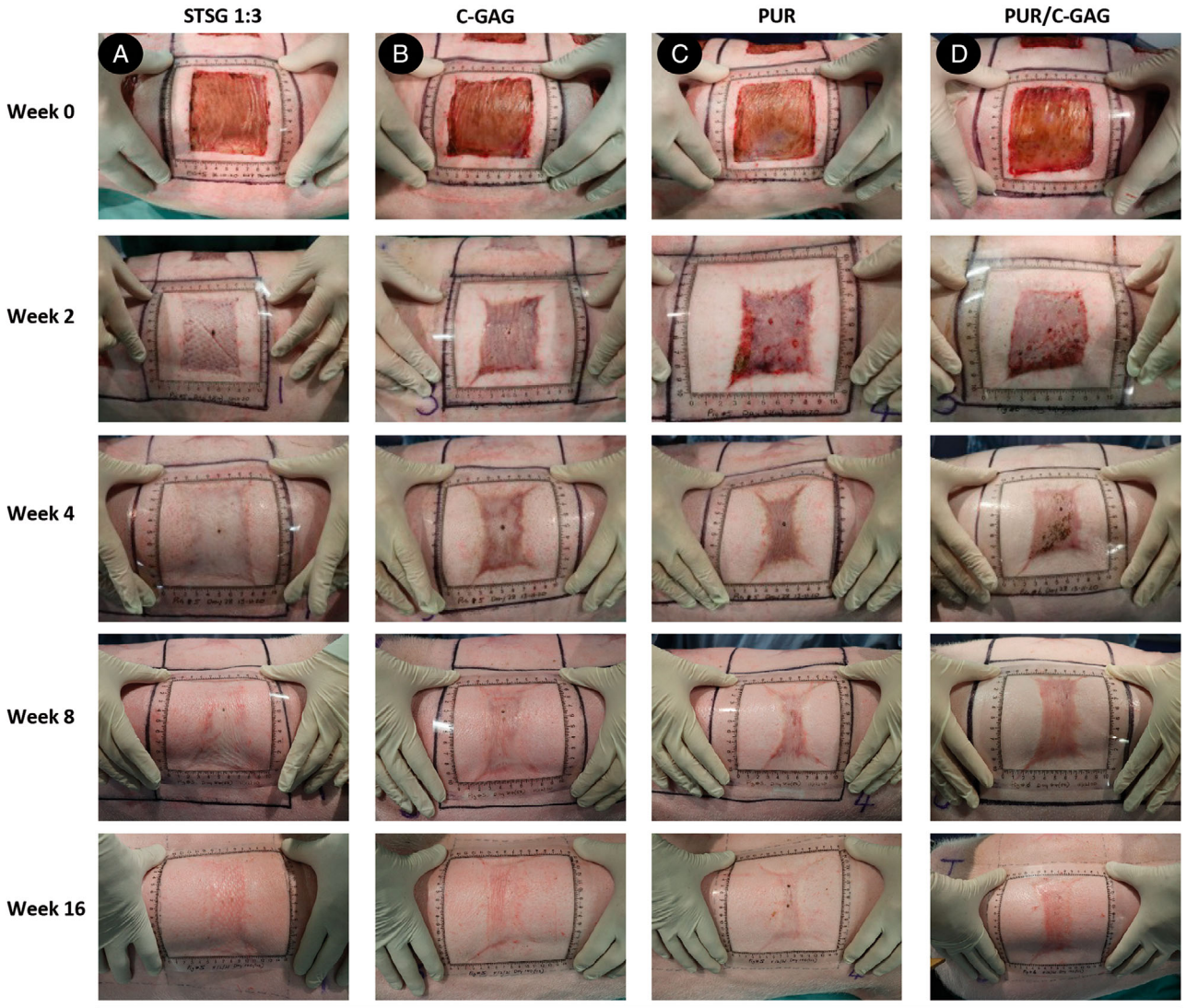

E Wound Contraction Day 0 – Day 112 Endpoint

STSG	C-GAG	PUR	PUR/C-GAG
44.17%	63.1%	67.87%	66.7%

FIGURE 1 Representative macroscopic images showing the progression of graft and skin substitute integration during weeks 0–16 post-transplant for each treatment condition. Meshed STSG (1:3) exhibited 44.2% contraction (column A), followed by the C-GAG substitute (63.1% column B), PUR/C-GAG 66.7% (column D) and the PUR substitute was on average the most contracted condition with 67.9% (column C). E, Percentage of contraction from day 0 after transplantation to day 112 endpoint.

wound area was estimated to be 22.2% smaller for the C-GAG relative to STSG (95% CI: 15.2–29.2). PUR/C-GAG was 26% (95% CI: 19.2–33.2) smaller, and PUR was 28% (95% CI: 21.9–35.9) smaller. From day 28 onwards, the wounds were considered 'closed' and stabilised to day 112 with no significant change for any condition.

Epithelialisation was measured from day 14 until completely healed (Figure 2B). The wound area and degree of contraction observed within the first 14–28 days relate to the percentage of epithelialisation and wound stabilisation. Within the test conditions, C-GAG and PUR/C-GAG substitutes showed on average the greatest percentage of epithelialisation at day 14 (87% and 88%, respectively). In reviewing conditions separately, two out of the three wounds for the polymer-based scaffolds were >90% healed at day 14. By day 112, most wound edges were indistinct and fused with the normal edge tissue.

An experienced burn surgeon performed the POSAS scoring system to assess the wound appearance by ordinal scoring. Due to a single reading and low numbers, results showed that the overall effect of condition on OSAS score was not significant ($Q(4) = 7.45$, $p = 0.113$). Table 1 shows the mean observer score outcomes. The

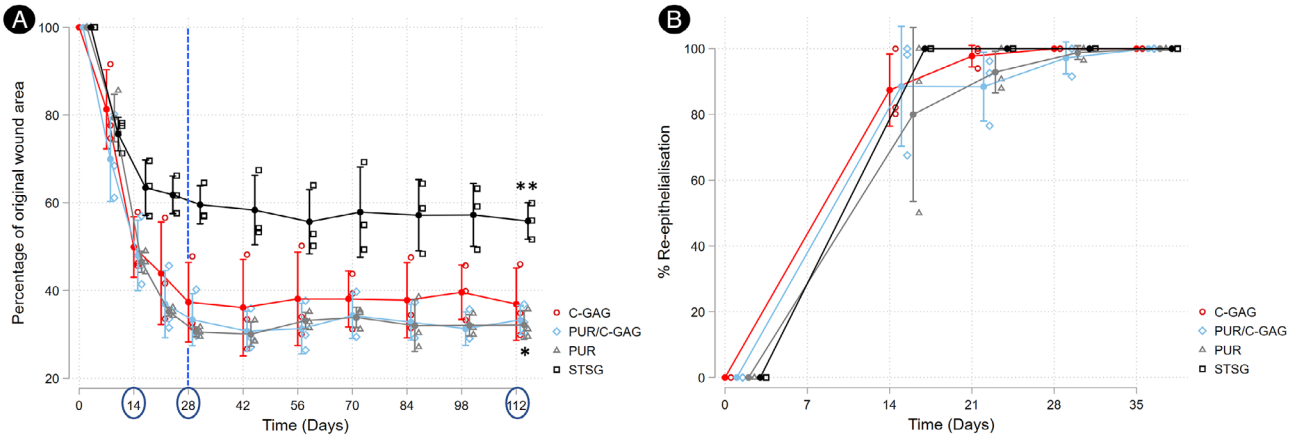

FIGURE 2 Wound percentage of original area and re-epithelialisation of the four test conditions over time shows the observed values and mean with standard deviation. (A) At 14 days post-transplant >80% of all wounds were re-epithelialised and by 28 days complete closure was obtained by secondary re-epithelialisation. At 28 days (dotted line) to 112 days, wound areas stabilised, and significant differences (**$p < 0.05$) were noted for all three skin substitutes compared to the STSG site at day 112, however there were no differences within each skin substitute condition (*$p > 0.05$). (B) Mean percentage of re-epithelialisation of test conditions over time until complete healing. No significant differences were found among the graft types after 14 days post-transplant ($p > 0.05$). Three biological replicates ($n = 3$) for each condition were analysed using a linear mixed effects model with Bonferroni correction.

STSG displayed the meshed graft pattern and contraction in all four corners with the beginning of a stellate appearance and a contour defect. The skin graft had a matte appearance and was more mature as it lacked colouration (pale) and had returned to uninjured skin colour. Although it was thinner, with less relief and supple, it had contracted in the head to tail perspective and expanded in the spine/flank with pig growth. The C-GAG substitute contracted quite markedly compared with the skin graft, and the majority was flush with the surface of the surrounding wound with small, raised contours and relatively pliable residual scar. They appeared redder, and the colour centrally indicated a wound not as mature, with capillary blanching and a shiny appearance. The PUR/C-GAG had a more matte appearance, less contraction and reduced scar thickness. There were minimal contour defects, and two out of the three displayed near full maturity with the least vascular pattern of pigmentation. The PUR wounds were flush with minimal contour defects; however, they were the most contracted with central bands of thickened scar and shiny mid-pink pigmentation.

3.3 | DermaLab results

The non-invasive multi-parameter skin analysis system, the DermaLab Combo, was used to relate the subjective observations noted above and provided more objective observations (Figure 3). At day 17, statistically significant differences in transepidermal water loss were found between the control STSG and all test conditions, the STSG did not differ from normal skin, (mean differences: STSG vs C-GAG 15.54 g/m^2/h [95% CI: 1.94–29.15], STSG vs. PUR/C-GAG 39.56 g/m^2/h [95% CI: 25.95–53.16] and STSG vs. PUR 29.11 g/m^2/h [95% CI: 15.50–42.72], respectively). However, the PUR site showed no difference from the C-GAG and PUR/C-GAG. All test conditions displayed higher values than normal skin at this early time point. With complete healing from day 28, all wound TEWL readings showed no changes among the groups for the study duration (Figure 3A). Additionally, the evaporative water loss decreased over time (day 17–112) for all skin substitute conditions ($p < 0.05$). The STSG showed no change over time as the site was re-epithelialised by day 14, with complete barrier function. For wound pigmentation (Figure 3B), melanin and erythema values differed significantly from normal skin and STSG to all test conditions on days 17, 28 and 56 for melanin and days 17 and 28 for erythema. By day 84, only the PUR containing scaffolds mean values (PUR, 30.57 ± 2.03 and PUR/C-GAG, 33.8 ± 6.13) differed with a higher melanin index than normal skin (23.68 ± 1.87). There were significant differences from days 17 to 112 for each graft condition ($p < 0.05$), representing a shift over time from dark to light (i.e., higher to lower MI). No differences were noted among the three test conditions for any time points for Melanin or Erythema Indices (Figure 3B,C). However, the Erythema Index (i.e., redness/vascularity)

TABLE 1 Showing the OSAS mean total score results for normal skin and all test conditions

Condition	*n*	Mean	SD	Median
Normal skin	3	6.0	0.0	6
PUR	3	23.3	8.0	24
C-GAG	3	25	2.7	26
HYBRID	3	22.3	12.1	18
STSG	3	19.3	4.2	18

Note: No significant differences were observed within the test conditions. Pairwise comparisons were assessed using Wilcoxon matched-pairs signed-rank tests.
Abbreviations: C-GAG, collagen-glycosaminoglycan; PUR, polyurethane; SD, standard deviation; STSG, split-thickness skin graft.

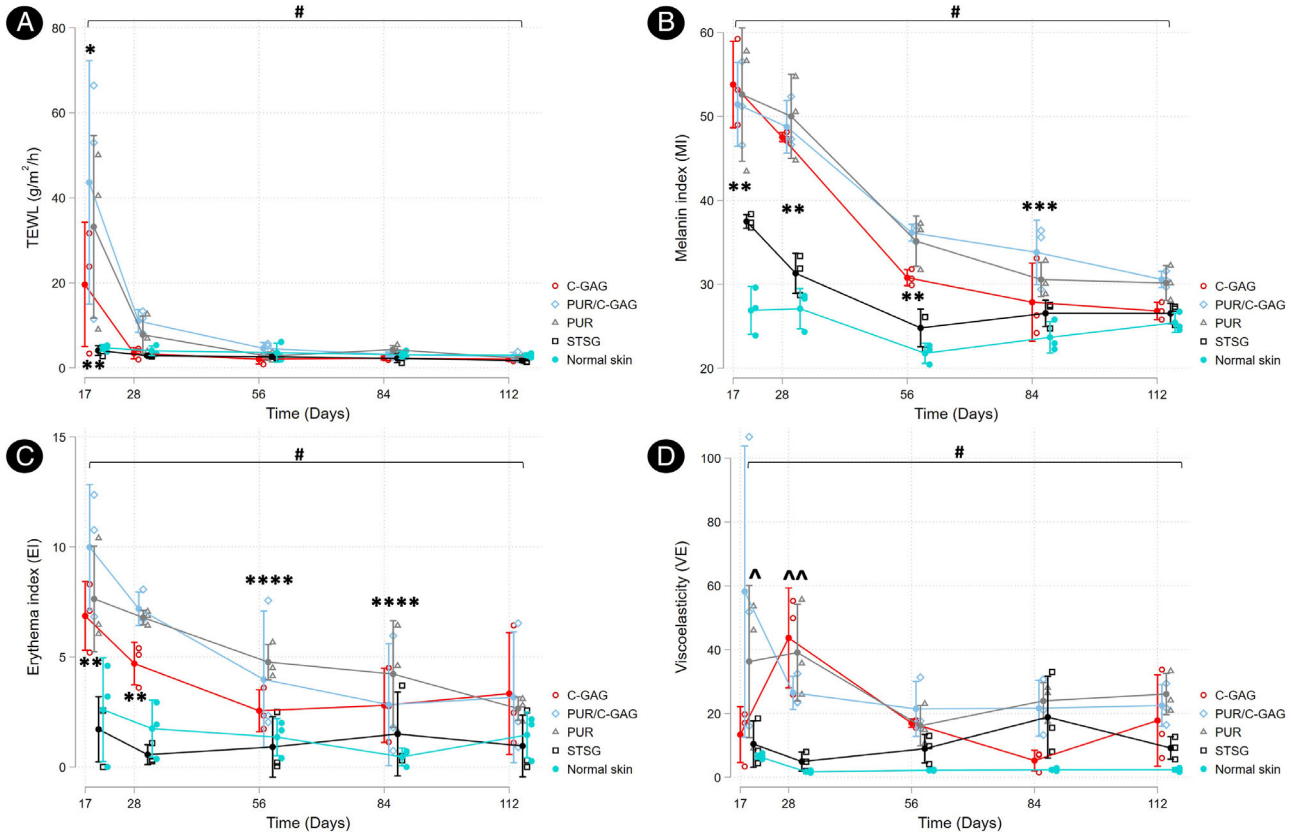

FIGURE 3 Results from the DermaLab with each biophysical wound assessment parameter graphed for all treatment conditions over time post-transplant. (A) Transepidermal water loss- TEWL (g/m^2/h), (B) Melanin Index (MI), (C) Erythema Index (EI), and (D) Viscoelasticity (VE). The observed values represent the means and standard deviations at respective time points. The mean differences were compared among conditions and over time. *p < 0.05 for comparisons among PUR/C-GAG, PUR, and C-GAG **p < 0.05 Normal skin compared to all conditions including STSG. ***p < 0.05 for comparisons of PUR/C-GAG, and normal skin, STSG, C-GAG. ****p < 0.05 PUR and normal skin. ^p < 0.05 Normal skin, STSG and both PUR-containing conditions. ^^p < 0.05 Normal skin, STSG and all test conditions. #p < 0.05 for comparisons among all test conditions at the indicated time points from days 17 to 112. Three biological replicates (n = 3) for each condition were analysed using a linear mixed effects model with Bonferroni correction.

of the PUR containing skin substitutes remained higher compared to the other conditions from day 17 (PUR/C-GAG 9.99 ± 2.85 and PUR 7.64 ± 2.4) through day 84 for the PUR (PUR 4.22 ± 2.42), by endpoint at day 112, no differences were observed among all conditions. The EI for all conditions decreased over time similarly to intact normal skin.

Measuring Young's Modulus on days 17, 28, 56, 84 and 112 confirmed wound parameters, that is, viscoelastic stretch under load, visco-elastic recovery after release of load and unrecovered deformation normalised by day 56 (Figure 3D). The PUR/C-GAG and PUR were the only conditions that differed from normal skin and STSG at d17, VE 51.61 (95% CI: 29.57–73.66) and 29.67 (95% CI: 3.1–51.72) respectively. Subsequent time points did not display this difference with STSG. Interestingly, all scaffolds showed an increase in VE readings on day 28. From this point, all test conditions displayed decreasing values, indicating some improvement of skin pliability over time. The ultrasound probe used to measure skin thicknesses only showed differences compared to normal skin and not within test conditions (p > 0.05) (data not shown).

3.4 | Microscopic evaluations

Biopsies post-delamination confirmed BTM integration (n = 12). The 2 mm inserted BTM after 28 days of integration with seal delamination decreased in thickness on average by half (964.5 µm ± 207.3). The BTM polymer layer resides below the surface of the skin at the interface between the connective tissue and the subcutaneous fat, with 21.5% remaining of the original polymer at 4.5 months post-implantation.

3.4.1 | Evaluation of histochemical staining

The structure of the wounds was evaluated by stained sections using Haematoxylin and Eosin (H&E). In Figure 4, row 1, representative images show normal epidermal morphology at day 112 post-transplant. Extrusion of the PUR was evident microscopically at day 10. An initial thick double epidermal layering effect with central PUR was evident within the PUR and PUR/C-GAG wounds at day 10, accentuating a very thick

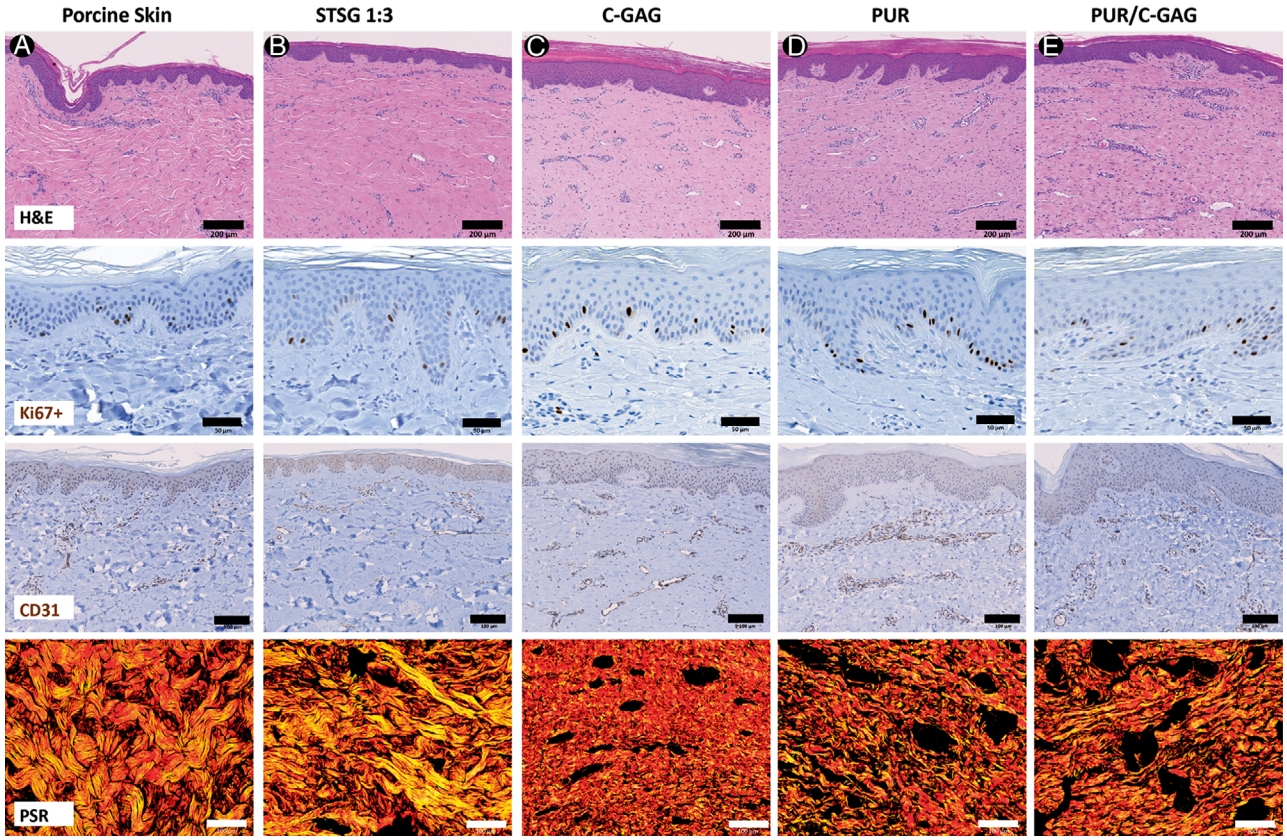

FIGURE 4 Representative histological images on day 112 post-transplantation. Haematoxylin and Eosin (H&E) row 1, Ki67-proliferative marker row 2, CD31-endothelial cell marker row 3 and Picrosirius red (PSR) stain row 4 for normal porcine skin (column A), and the four test conditions, skin graft (STSG-column B), C-GAG (column C), PUR (column D) and hybrid PUR/C-GAG (column E). The collagen structure was visualised using PSR under polarised light. Scale bar: 200 μm row 1, 50 μm row 2, 100 μm row 3 and 4

hyperproliferative epidermis. By day 112, the stratified epidermal layers for all test conditions appeared similar to STSG (Figure 4). All wounds presented with typical epidermal morphology, well-defined rete ridges, columnar basal cells and keratin layers by day 112.

The hyperproliferative epidermal phenotype observed at day 10 was resolved by day 112, displaying a regular expression of Ki67 within the basal keratinocytes (Figure 4, row 2). Revascularisation of the tissue was confirmed by staining with CD31 endothelial cell marker (Figure 4, row 3). Blood vessel density increased at the early stages of healing for all test conditions compared with normal skin.

The initial granulation layer was highly cellular, populated with numerous vessels and inflammatory cells. The dermal structure was then assessed for collagen deposition and morphology using picrosirius red stain (Figure 4, row 4). Type I collagen predominates in all sections (red/yellow staining), shown as thick, dense bundles in the control tissues (Figure 4, row 4). At early time points for the test conditions, the collagen fibres were thin with minimal collagen deposition (i.e., reduced red). The C-GAG presented thin, compact/dense bundles compared to the PUR and hybrid, which contained a less dense, looser, randomly organised fibre orientation. The three test scaffolds illustrated black areas within the tissue, consistent with a lower density of collagen fibres (Figure 4C–E, row 4) compared with either the control STSG or normal porcine skin (Figure 4A,B, row 4) at day 112. The degree of collagen deposition increased over time for all wound conditions, with fibroblasts actively depositing and producing new collagen. All comprised qualitatively less collagen than normal skin, donor site and STSG control site.

At day 112 post-transplant epidermal structural integrity was confirmed by staining for keratin marker, cytokeratin 14 (K14), this showed K14 positive cells for all test and control conditions within the basal layers (Figure 5, row 1). Basement membrane markers indicated epidermal-dermal structure integrity with positive staining for collagen IV, collagen VII and integrin α6 (CD49f) (Figure 5, rows 2–4).

4 | DISCUSSION

The hybrid scaffold was successfully fabricated to fill the pores of the PUR with collagen-GAG. It provided and facilitated a surface that promoted morphogenesis of the cells into a dermal-epidermal skin substitute, with good in vitro and handling properties. Data presented in this study demonstrate all three test scaffolds, and subsequent skin substitutes allowed for tissue integration and enabled stable wound closure. This study, in addition, confirms the advantages and disadvantages of these materials. The split-thickness skin autograft is considered the prevailing standard of care for wound coverage in extensive

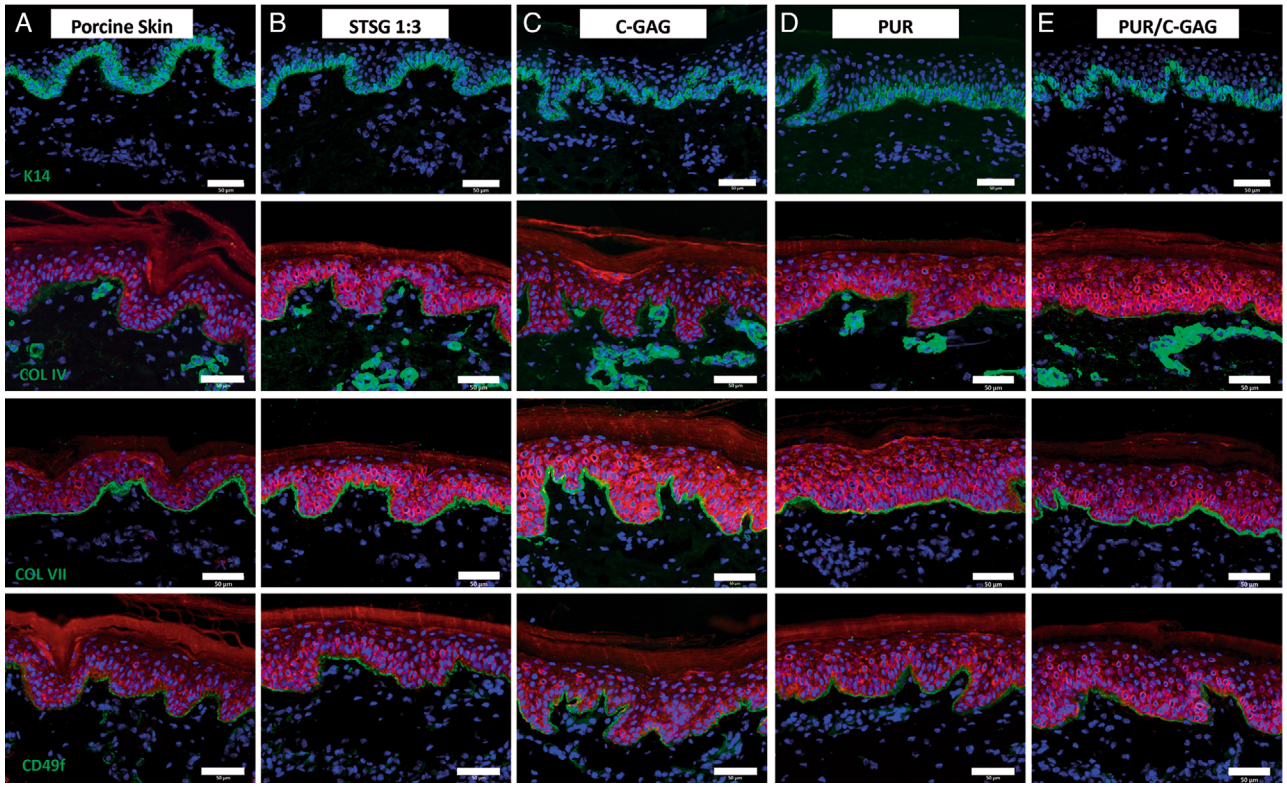

FIGURE 5 Representative immunohistological images of normal porcine skin and test conditions at 112 days post-transplantation showing epidermal and basement membrane confirmation. Cytokeratin 14 row 1, Collagen IV row 2, Collagen VII row 3 and Integrin α6 (CD49f) row 4. Column a represents porcine normal skin, column b STSG, column c C-GAG, column d PUR and column e PUR/C-GAG. Red staining for wide spectrum cytokeratin, Green staining depicts relevant maker, DAPI nuclei stain. Scale bar: 50 μm

full-thickness injuries. The meshed 1:3 skin autograft was a control condition and resulted in a superior outcome over the test skin substitutes regarding wound size and resemblance to intact, normal skin. However, the limitations of this treatment option is its paucity and aesthetics (characteristic mesh interstices and concave appearance),[31] not unlike those observed in this study.

The second-largest wound (C-GAG) and the largest of the three test conditions re-epithelialised early, with an apparent thicker dermis but a loose, 'wrinkling' appearance by study end. The inherent contraction of the C-GAG template during skin substitute fabrication increased the quantities required, potentially increasing handling and future set up costs for clinical use.[32] In an attempt to reduce contraction, a previous study by Powell and Boyce demonstrated a combination C-GAG with a PCL component improving its mechanical properties.[33] The PUR/C-GAG hybrid also reduced in vitro contraction with superior thickness and handling properties. Conversely, the in vivo PUR loss and extrusion reduced mechanical support and resulted in smaller wounds with increased contraction. This PUR 'crusting' phenomenon has been reported previously.[25] The hybrid inconsistencies noted with the C-GAG fabrication and cross-linking produced non-contiguous epithelium in vitro attributing to areas showing delayed post-polymer 'spitting'.

The patient observer scar assessment scale (POSAS) is becoming the accepted measure of scar quality.[34] Using this method enabled valuable subjective observations of the wounds, and for future studies, increased observer scores may allow for data correlation with the DermaLab, enabling multiple assessments and conclusions of the wound/scar.[35,36] TEWL confirmed wound closure and barrier function which could be associated with the percentage of re-epithelialisation and closure rates. The TEWL values stabilised to normal skin values from day 31 to 112, demonstrating continual epidermal barrier function with the outermost layer, the stratum corneum.[37] Immunohistochemical staining confirmed that the major constituents of the basement membrane which are fundamental in attaching the epidermal cells to the underlying extracellular matrix are present. All conditions demonstrated, collagen IV (BM stability), collagen VII (BM anchoring fibrils), and CD49f (binding of integrin α-6 to BM), markers essential to maintain basement membrane formation-function and skin homeostasis.[38]

The skin's viscoelasticity is mainly determined by the ECM and the presence of collagen and elastin fibres, enabling the skin to return to its prior shape after stretch. An increase in viscoelasticity values—high MPa was initially observed for all grafts at early time points (day 17–28), presenting a stiffer, less pliable graft. The increase in PUR and PUR/C-GAG elasticity values may be related to the proportion of collagen III at this early time point. In common with a previous study,[39] a peak in collagen type III alpha chain (COL3A1) expression was observed at 28 days in a hypertrophic scar porcine wound model for

>1.9 mm deep dermatome injuries,[39] suggesting PUR containing substitutes initiated a similar healing process. Once in the remodelling phase, the VE values decreased over time, improving the pliability of the skin. Although they never achieved intact skin values, they also did not differ from STSG by study end. This has previously been noted when autograft and bilayered skin substitutes were evaluated in 14 burned patients.[40] Furthermore, Boyce and colleagues reported the scar pliability of skin substitutes (collagen-based) were similar to autograft 1 year after treatment in burn patients.[41] In this study, the C-GAG presented increased collagen content organised into thinner, more compact fibres with an apparent thicker dermis, suggesting the C-GAG grafts matured earlier[8] with similar viscoelastic properties to skin autograft.

Since the skin of dominant white pigs lack melanocytes[42] the pigmentation observed in the porcine wounds reflects the degree of inflammation and erythema of a skin injury. Therefore, the elevated melanin index and vascularity values at early time points were consistent with neovascularisation and the proliferation phase of wound healing,[43] restoring to baseline with graft stabilisation by study end for all except the PUR grafts. All biomaterial implants are considered foreign bodies. The minimal change in erythema in the PUR grafts from transplant to the study end, suggests the wound remained (red) in an active inflammatory state from a retention of polymer (foreign body), thus prolonging maturation.[43] The expression of CD31+ vessels confirmed an ingrowth of vascular supply with an increase in MVD during the early inflammatory and proliferative phases for all wounds. An increase in matrix deposition with a decrease in vascularisation at day 112 suggests regulation of angiogenesis in the remodelling phase. It has been previously reported that engineered skins in vitro have a hyperproliferative phenotype and, within weeks, is normalised after grafting.[17,44] The present study also showed this characteristic, normalising to control STSG levels by study end with no detrimental effect on engraftment and no overexpression of Ki67.

Several limitations of this study are noteworthy; the DermaLab-ultrasound provided some difficulties. The probe has a limiting penetration capacity of 3.4 mm, and considering post histological sections showed greater than this, Young's Modulus elasticity values may have been affected.[36] Using the mean of repeated measurements to interpret the DermaLab results correctly is highly recommended where feasible.[45] The requirement of a time delay between each repetition, the curvature of the animal and wound shape and size, only enabled the collection of one measurement with the elasticity probe. The use of the DermaLab has shown potential for its use in large animal cutaneous wound healing models providing a non-invasive, standardised technique for multiple wound parameters and, with repetition, is a promising all-in-one instrument. Another study constraint includes sample size. Porcine wound studies are limited to the number of wounds per pig, handling capacity and cost.[46,47] Histological variability can be produced upon processing, staining and analysing sections and the heterogeneity within the field of graft upon sampling is a consideration.

Overall, based on these data, the three biopolymer scaffolds used to fabricate engineered skins produced a permanent skin replacement, promoting wound closure with epithelialisation and vascularisation with similar biophysical properties to the skin autograft. Therefore, taking into consideration their disadvantages and advantages, any one of these formulations would reduce the requirement for skin autografts, and the plausibility of laboratory-based skin as a replacement is feasible.[5,48] A trending effect was observed in this preliminary study, with prospective studies being required to decrease conditions to allow greater sample sizes in order to provide stronger statistical analysis and conclusions. However, the PUR/C-GAG hybrid has shown potential as a suitable biomaterial scaffold for fabricating skin substitutes, resolving the inherent concerns with collagen (i.e., contraction) and PURs (i.e., porosity). This material would significantly impact extensive burns and other acute and chronic wounds that would benefit therapeutically to reduce donor site harvesting, numbers of skin autografting procedures, and long-term morbidity from scars.

AUTHOR CONTRIBUTIONS

Bronwyn L. Dearman wrote the manuscript. All authors provided critical feedback and reviewed and approved the final version of the manuscript.

ACKNOWLEDGEMENTS

This project was supported by Lifetime Support Authority. We thank LARIF SAHMRI Animal facility technicians, the University of Adelaide Histology, Microscopy and Statistician Departments. We gratefully acknowledge the Skin Engineering Laboratory and Renal laboratory personnel for assistance with culturing and staining techniques. Thanks and much appreciation to the Engineered Skin Laboratory at the University of Cincinnati for assistance and advice with the hybrid scaffold fabrication. Open access publishing facilitated by The University of Adelaide, as part of the Wiley - The University of Adelaide agreement via the Council of Australian University Librarians.

DATA AVAILABILITY STATEMENT

The data that support the findings of this study are available from the corresponding author upon request.

ORCID

Bronwyn L. Dearman https://orcid.org/0000-0001-8804-8401
Steven T. Boyce https://orcid.org/0000-0002-7683-7646

REFERENCES

1. Dearman BL, Boyce ST, Greenwood JE. Advances in skin tissue bioengineering and the challenges of clinical translation. *Front Surg*. 2021;8:640879.
2. Yannas IV, Burke JF, Huang C, Gordon PL. Correlation of in vivo collagen degradation rate with in vitro measurements. *J Biomed Mater Res*. 1975;9(6):623-628.
3. Boyce ST, Christianson DJ, Hansbrough JF. Structure of a collagen-GAG dermal skin substitute optimized for cultured human epidermal keratinocytes. *J Biomed Mater Res*. 1988;22(10):939-957.
4. Yannas IV, Burke JF. Design of an artificial skin. I. Basic design principles. *J Biomed Mater Res*. 1980;14(1):65-81.
5. Boyce ST, Simpson PS, Rieman MT, et al. Randomized, paired-site comparison of autologous engineered skin substitutes and split-

thickness skin graft for closure of extensive, full-thickness burns. *J Burn Care Res*. 2017;38(2):61-70.
6. Vaissiere G, Chevallay B, Herbage D, Damour O. Comparative analysis of different collagen-based biomaterials as scaffolds for long-term culture of human fibroblasts. *Med Biol Eng Comput*. 2000;38(2):205-210.
7. Dearman BL, Greenwood JE. Scale-up of a composite cultured skin using a novel bioreactor device in a porcine wound model. *J Burn Care Res*. 2021;42(6):1199-1209.
8. Banakh I, Cheshire P, Rahman M, et al. A comparative study of engineered dermal templates for skin wound repair in a mouse model. *Int J Mol Sci*. 2020;21(12):4508.
9. Harley BAC, Gibson LJ. In vivo and in vitro applications of collagen-GAG scaffolds. *Chem Eng J*. 2008;137(1):102-121.
10. Eskandarinia A, Kefayat A, Agheb M, et al. A novel bilayer wound dressing composed of a dense polyurethane/propolis membrane and a biodegradable polycaprolactone/gelatin nanofibrous scaffold. *Sci Rep*. 2020;10(1):3063.
11. Anjum F, Agabalyan NA, Sparks HD, Rosin NL, Kallos MS, Biernaskie J. Biocomposite nanofiber matrices to support ECM remodeling by human dermal progenitors and enhanced wound closure. *Sci Rep*. 2017;7(1):10291.
12. Sadeghi-Avalshahr AR, Nokhasteh S, Molavi AM, Mohammad-Pour N, Sadeghi M. Tailored PCL scaffolds as skin substitutes using sacrificial PVP fibers and collagen/chitosan blends. *Int J Mol Sci*. 2020;21(7):2311.
13. Sadeghi AR, Nokhasteh S, Molavi AM, Khorsand-Ghayeni M, Naderi-Meshkin H, Mahdizadeh A. Surface modification of electrospun PLGA scaffold with collagen for bioengineered skin substitutes. *Mater Sci Eng C Mater Biol Appl*. 2016;66:130-137.
14. Knight E, Murray B, Carnachan R, Przyborski S. Alvetex®: polystyrene scaffold technology for routine three dimensional cell culture. *Methods Mol Biol*. 2011;695:323-340.
15. Khalili S, Nouri Khorasani S, Razavi M, Hashemi Beni B, Heydari F, Tamayol A. Nanofibrous scaffolds with biomimetic structure. *J Biomed Mater Res A*. 2018;106(2):370-376.
16. Dehghani F, Annabi N. Engineering porous scaffolds using gas-based techniques. *Curr Opin Biotechnol*. 2011;22(5):661-666.
17. Paul M, Kaur P, Herson M, Cheshire P, Cleland H, Akbarzadeh S. Use of clotted human plasma and aprotinin in skin tissue engineering: a novel approach to engineering composite skin on a porous scaffold. *Tissue Eng Part C Methods*. 2015;21(10):1098-1104.
18. Solovieva EV, Teterina AY, Klein OI, Komlev VS, Alekseev AA, Panteleyev AA. Sodium alginate-based composites as a collagen substitute for skin bioengineering. *Biomed Mater*. 2020;16(1):015002.
19. Solovieva EV, Fedotov AY, Mamonov VE, Komlev VS, Panteleyev AA. Fibrinogen-modified sodium alginate as a scaffold material for skin tissue engineering. *Biomed Mater*. 2018;13(2):025007.
20. Chanda A, Adhikari J, Ghosh A, et al. Electrospun chitosan/polycaprolactone-hyaluronic acid bilayered scaffold for potential wound healing applications. *Int J Biol Macromol*. 2018;116:774-785.
21. Kim H, Son D, Choi TH, et al. Evaluation of an amniotic membrane-collagen dermal substitute in the management of full-thickness skin defects in a pig. *Arch Plast Surg*. 2013;40(1):11-18.
22. Türkkan S, Atila D, An A, Ae T. Fabrication of functionalized citrus pectin/silk fibroin scaffolds for skin tissue engineering. *J Biomed Mater Res B Appl Biomater*. 2018;106:2625-2635.
23. Sierra-Sanchez A, Fernandez-Gonzalez A, Lizana-Moreno A, et al. Hyaluronic acid biomaterial for human tissue-engineered skin substitutes: preclinical comparative in vivo study of wound healing. *J Eur Acad Dermatol Venereol*. 2020;34(10):2414-2427.
24. Kim JW, Kim MJ, Ki CS, Kim HJ, Park YH. Fabrication of bi-layer scaffold of keratin nanofiber and gelatin-methacrylate hydrogel: implications for skin graft. *Int J Biol Macromol*. 2017;105(Pt 1):541-548.
25. Dearman BL, Stefani K, Li A, Greenwood JE. "Take" of a polymer-based autologous cultured composite "skin" on an integrated temporizing dermal matrix: proof of concept. *J Burn Care Res*. 2013;34(1):151-160.
26. Dearman BL, Li A, Greenwood JE. Optimization of a polyurethane dermal matrix and experience with a polymer-based cultured composite skin. *J Burn Care Res*. 2014;35(5):437-448.
27. Powell HM, Boyce ST. EDC cross-linking improves skin substitute strength and stability. *Biomaterials*. 2006;27(34):5821-5827.
28. Supp DM, Hahn JM, Lloyd CM, et al. Light or dark pigmentation of engineered skin substitutes containing melanocytes protects against ultraviolet light-induced DNA damage in vivo. *J Burn Care Res*. 2020;41:751-760.
29. Hassiotis S, Manavis J, Blumbergs PC, et al. Lysosomal LAMP1 immunoreactivity exists in both diffuse and neuritic amyloid plaques in the human hippocampus. *Eur J Neurosci*. 2018;47(9):1043-1053.
30. Draijers LJ, Tempelman FRH, Botman YAM, et al. The patient and observer scar assessment scale: a reliable and feasible tool for scar evaluation. *Plast Reconstr Surg*. 2004;113(7):1960-1965.
31. Shevchenko RV, James SL, James SE. A review of tissue-engineered skin bioconstructs available for skin reconstruction. *J R Soc Interface*. 2010;7(43):229-258.
32. Powell HM, Boyce ST. Wound closure with EDC cross-linked cultured skin substitutes grafted to athymic mice. *Biomaterials*. 2007;28(6):1084-1092.
33. Powell HM, Boyce ST. Engineered human skin fabricated using electrospun collagen-PCL blends: morphogenesis and mechanical properties. *Tissue Eng Part A*. 2009;15(8):2177-2187.
34. Carriere ME, Kwa KAA, de Haas LEM, et al. Systematic review on the content of outcome measurement instruments on scar quality. *Plast Reconstr Surg Glob Open*. 2019;7(9):e2424.
35. Gankande TU, Duke JM, Danielsen PL, DeJong HM, Wood FM, Wallace HJ. Reliability of scar assessments performed with an integrated skin testing device – the DermaLab Combo®. *Burns*. 2014;40(8):1521-1529.
36. Peperkamp K, Verhulst AC, Tielemans HJP, Winters H, van Dalen D, Ulrich DJO. The inter-rater and test-retest reliability of skin thickness and skin elasticity measurements by the DermaLab Combo in healthy participants. *Skin Res Technol*. 2019;25(6):787-792.
37. Suetake T, Sasai S, Zhen Y-X, Ohi T, Tagami H. Functional analyses of the stratum corneum in scars: sequential studies after injury and comparison among keloids, hypertrophic scars, and atrophic scars. *Arch Dermatol*. 1996;132(12):1453-1458.
38. Supp DM, Hahn JM, Combs KA, et al. Collagen VII expression is required in both keratinocytes and fibroblasts for anchoring fibril formation in bilayer engineered skin substitutes. *Cell Transplant*. 2019;28(9–10):1242-1256.
39. Blackstone BN, Kim JY, McFarland KL, et al. Scar formation following excisional and burn injuries in a red Duroc pig model. *Wound Repair Regen*. 2017;25(4):618-631.
40. Germain L, Larouche D, Nedelec B, et al. Autologous bilayered self-assembled skin substitutes (SASSs) as permanent grafts: a case series of 14 severely burned patients indicating clinical effectiveness. *Eur Cell Mater*. 2018;36:128-141.
41. Boyce ST, Supp AP, Wickett RR, Hoath SB, Warden GD. Assessment with the dermal torque meter of skin pliability after treatment of burns with cultured skin substitutes. *J Burn Care Rehabil*. 2000;21(1):55-63.
42. Müller S, Wanke R, Distl O. Inheritance of melanocytic lesions and their association with the white colour phenotype in miniature swine. *J Anim Breed Genet*. 2001;118(4):275-283.
43. Landen NX, Li D, Stahle M. Transition from inflammation to proliferation: a critical step during wound healing. *Cell Mol Life Sci*. 2016;73(20):3861-3885.

44. Smiley AK, Klingenberg JM, Boyce ST, Supp DM. Keratin expression in cultured skin substitutes suggests that the hyperproliferative phenotype observed in vitro is normalized after grafting. *Burns*. 2006; 32(2):135-138.
45. Anthonissen M, Daly D, Fieuws S, et al. Measurement of elasticity and transepidermal water loss rate of burn scars with the Dermalab®. *Burns*. 2013;39(3):420-428.
46. Sami DG, Heiba HH, Abdellatif A. Wound healing models: a systematic review of animal and non-animal models. *Wound Med*. 2019; 24(1):8-17.
47. Pastar I, Liang L, Sawaya AP, et al. Preclinical models for wound-healing studies. In: Marques AP, Pirraco RP, Cerqueira MT, Reis RL, eds. *Skin Tissue Models for Regenerative Medicine*. Elsevier; 2018: 223-253.
48. Schiestl C, Meuli M, Vojvodic M, et al. Expanding into the future: combining a novel dermal template with distinct variants of autologous cultured skin substitutes in massive burns. *Burns*. 2021; 5(3):145-153.

SUPPORTING INFORMATION

Additional supporting information can be found online in the Supporting Information section at the end of this article.

How to cite this article: Dearman BL, Boyce ST, Greenwood JE. Comparison of biopolymer scaffolds for the fabrication of skin substitutes in a porcine wound model. *Wound Rep Reg*. 2023;31(1):87-98. doi:10.1111/wrr.13059